# Electronic Supplementary Information

## Pillar[3]trianglamines: Deeper Cavity Triangular Macrocycles for Selective Hexene Isomers Separation

Yanjun Ding,[1] Lukman O. Alimi,[1] Jing Du,[2] Bin Hua,[1] Avishek Dey,[1] Pei Yu[1] and Niveen M. Khashab[1]*

[1] Smart Hybrid Materials (SHMs) Laboratory, Advanced Membranes and Porous Materials Center, King Abdullah University of Science and Technology (KAUST), Thuwal 23955-6900, Kingdom of Saudi Arabia.

[2]Key Laboratory of Polyoxometalate and Reticular Material Chemistry of Ministry of Education, Faculty of Chemistry, Northeast Normal University, Changchun, 130024, China.

## 1. Experimental Procedures

***1.1. Materials.*** All chemicals were purchased from commercial sources and used as received.

***1.2. Synthesis of trianglamine TA.*** Trianglamine **TA** was prepared according to previous report.[1] $^1$H NMR (400 MHz, Chloroform-d) δ 7.15 (s, 2H), 4.07 (d, *J* = 14.0 Hz, 1H), 3.28 (s, 1H), 3.16 (d, *J* = 14.0 Hz, 1H), 2.30 – 2.28 (m, 1H), 2.04 – 2.02 (m, 1H), 1.84 – 1.82 (m, 1H), 1.33 – 1.27 (m, 2H); $^{13}$C NMR (101 MHz, Chloroform-d) δ 138.04, 127.58, 69.13, 57.68, 29.44, 24.59. HRMS (ESI) calcd for $C_{45}H_{61}N_6$ [(M+H)$^+$]: 685.4958, Found: 685.5024.

***1.3. Synthesis of ligand Da-A.*** A solution of **Da** (498.4 mg, 3.0 mmol) and allyl bromide (907.4 mg, 7.5 mmol) in acetonitrile (50 mL) was heated at reflux with powdered $K_2CO_3$ (1.66 g, 12 mmol) for 4 h. The solvent was evaporated and the residue was dissolved in $CH_2Cl_2$ and extracted with aqueous $Na_2CO_3$ (5%). The organic phase was dried over $NaSO_4$, evaporated and dried in vacuo to get the crude product in 83% yield, which was directly used in the next step. $^1$H NMR (400 MHz, Chloroform-d) δ 10.53 (s, 2H), 7.44 (s, 2H), 6.06 (ddt, J = 17.2, 10.5, 5.2 Hz, 2H), 5.44 (dq, J = 17.2, 1.5 Hz, 2H), 5.34 (dq, J = 10.6, 1.4 Hz, 2H), 4.67 (dt, J = 5.2, 1.6 Hz, 4H); $^{13}$C NMR (101 MHz, Chloroform-d) δ 189.28, 154.90, 132.22, 129.51, 118.62, 112.29, 69.93.

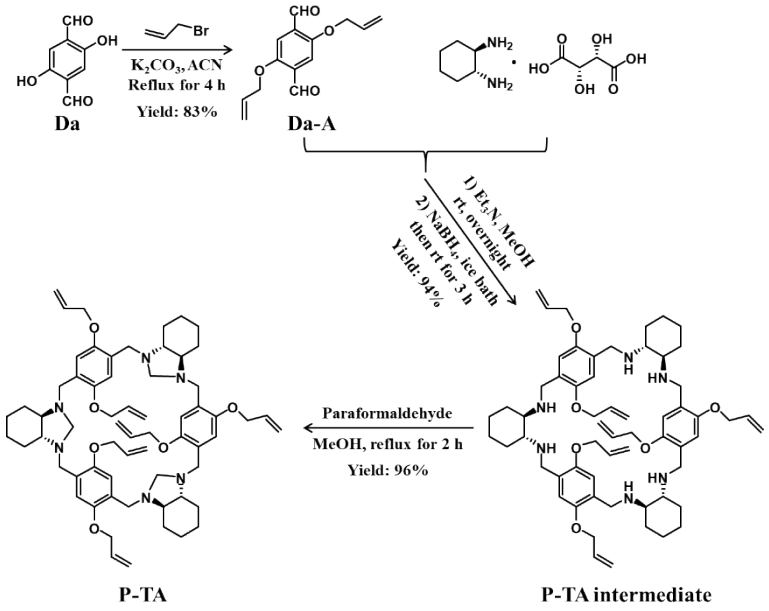


**Scheme S1.** Synthetic scheme of pillar[3]trianglamine **P-TA**.

***1.4. Synthesis of P-TA intermediate.*** A mixture of (R, R)-(+)-1,2-Diaminocyclohexane L-Tartrate (528.6 mg, 2.0 mmol), **Da-A** (492.5 mg, 2.0 mmol), MeOH (20 mL) and triethylamine (0.7 mL) were stirred at room temperature overnight. The mixture was cooled in an ice bath and sodium borohydride (228 mg, 6 mmol) was added over one hour. After the system had been stirred for a further three hours at room temperature, the solvents were removed in vacuo and the residue was extracted with dichloromethane and aqueous sodium carbonate (5%). The organic solution was dried over $NaSO_4$, evaporated and dried in vacuo. Trianglamine **P-TA intermediate** was obtained in a yield of 94%. HRMS (ESI) calcd for $C_{60}H_{85}N_6O_6$ [(M+H)$^+$]: 985.6531, Found: 985.6526.

***1.5. Synthesis of Pillared Trianglamine P-TA.*** **P-TA intermediate** (492.7 mg, 0.5 mmol) and paraformaldehyde (180 mg, 6 mmol) in $CH_3OH$ (10 mL) was stirred at 70 °C for 2 h. The solvent was evaporated and the residue was dissolved in $CH_2Cl_2$ and extracted with aqueous $Na_2CO_3$ (5%). The organic phase was dried over $NaSO_4$, evaporated and dried in vacuo to get the crude product in 96% yield. Crude product was purified via crystallization from dichloromethane. $^1$H NMR (400 MHz, Chloroform-d) δ 6.93 (s, 6H), 5.95 (ddt, J = 17.3, 10.4, 5.1 Hz, 6H), 5.28 (dq, J = 17.3, 1.7 Hz, 6H), 5.10 (dq, J = 10.6, 1.6 Hz, 6H), 4.42 (d, J = 1.6 Hz, 12H), 3.71 (d, J = 14.7 Hz, 6H), 3.53 (d, J = 14.6 Hz, 6H), 3.28 (s, 6H), 2.35 – 2.33 (m, 6H), 2.04 – 2.02 (m, 6H), 1.83 – 1.81 (m, 6H), 1.31 – 1.25 (m, 12H); $^{13}$C NMR (101 MHz, Chloroform-d) δ 150.12, 133.94, 127.09, 117.01, 113.23, 77.94, 69.60, 69.30, 51.22, 29.63, 24.66. HRMS (ESI) calcd for $C_{63}H_{85}N_6O_6$ [(M+H)$^+$]: 1021.6531, Found: 1021.6722.

***1.6. Single Crystal Growth.*** Single crystals of the pillared trianglamine **P-TA** were grown by slow evaporation of dichloromethane solution at room temperature. Single crystals of **1-He@P-TA** were obtained as follows: firstly mixed **P-TA** with 1-He, then sonicated it for 10 min and filtered the mixture through a PTFE membrane (220 nm) to get a clear solution, finally colorless single crystals appeared by slow evaporation of 1-He over several days. Single crystals of ***trans*-3-He@P-TA** were grown via a vapor diffusion

method: **P-TA** dissolved in $CHCl_3$ in a small vial was placed in a large vial containing *trans*-3-He to allow *trans*-3-He diffusion into the $CHCl_3$ solution.

***1.7. Adsorption Material Activation.*** The desolvated **P-TA** crystals were prepared under vacuum at 120 ℃ overnight. The activated adsorptive separation materials (activated **P-TA**) after adsorption could be regenerated to release the adsorbed guests upon heating at 90 ℃ under vacuum overnight, and the released guests could be collected via a condensation setup.

***1.8. Adsorption Experiments for linear hexene isomers vapor.*** An open 5 mL vial containing 10 mg of adsorbent was placed in a sealed 20 mL vial containing 1 mL of solvents (1-He, *trans*-3-He or an equimolar mixture of 1-He and *trans*-3-He) at room temperature. The uptake capacity of adsorbents was measured at different time intervals by completely dissolving the samples in $CDCl_3$ and measuring the ratio of 1-He or *trans*-3-He by $^1$H NMR, respectively. Uptake capacity values were determined from the ratio of each isomer peaks using $^1$H NMR and GC following literature protocols.[2]

## 2. Methods

***2.1. Solution NMR.*** NMR spectra were recorded on Bruker-400 (400 MHz for $^1$H; 101 MHz for $^{13}$C) instruments internally referenced to $SiMe_4$ signal.

***2.2. Thermogravimetric Analysis.*** Thermogravimetric analysis (TGA) was carried out using a TGA Q50 analyzer (TA Instruments) with an automated vertical overhead thermobalance. The samples were heated at 10 °C/min from 25 to 800 °C using $N_2$ as the protective gas.

***2.3. Nitrogen Adsorption Experiment.*** Low-pressure gas adsorption measurement was performed on a Micromeritics Accelerated Surface Area and Porosimetry System (ASAP) 2020 surface area analyzer. Samples were degassed under dynamic vacuum for 12 h at 60 °C prior to each measurement. $N_2$ isotherms were measured using a liquid nitrogen bath (77 K).

***2.4. Powder X-Ray Diffraction.*** Powder X-ray diffraction (PXRD) patterns were obtained using a D8 ADVANCE Twin X-ray diffractometer (40 KV, 40 mA) with the Cu Kα radiation (λ = 1.54178 Å). Data were measured over the range of 3−40° in 2°/min steps.

***2.5. Single Crystal X-ray Diffraction.*** Single crystal X-ray diffraction data were recorded on a Bruker D8 Venture equipped with a digital camera diffractometer using graphite-monochromated Cu Kα (λ= 1.54178 Å) or Mo Kα (λ= 1.54178 Å) radiation for the crystal structures. Raw data were integrated using Bruker AXS SAINT software and absorption corrections were applied using SADABS.[3,4] All structures were solved with the ShelXT structure solution program using Intrinsic Phasing and refined with the ShelXL refinement package using Least Squares minimization operated in the OLEX2 interface.[5] All non-hydrogen atoms were refined anisotropically. In the final refinement, a twin law (TWIN -1 -1 0 0 1 0 0 0 -1 2; BASF = 0.12) was required for the structural refinement of **1-He@P-TA**. Based on theanalysis of $^1$H NMR and TGA as well as the solvent mask calculation results, the asymmetric unit contains one unit of **P-TA** and one unit of 1-He in the **1-He@P-TA**; While *trans*-3-He molecules sit inside the intrinsic cavity of **P-TA** with 0.5 occupancy in the ***trans*-3-He@P-TA**. The hydrogen atoms on organic carbon atoms were fixed in calculated positions. Crystal data and structural refinement for **1-He@P-TA** and ***trans*-3-He@P-TA** are listed in Table S2.

***2.6. Gas Chromatography.*** Gas Chromatographic (GC) Analysis: GC measurements were carried out using a J&W (122-1364) instrument configured with an FID detector and a DB-624 column (60 m × 0.25 mm × 1.4 μm). The following GC method was used: the oven was programmed from 40 °C ramped in 10 °C/min increments to 240 °C with 26 min hold. The total run time was 50 min and the injection temperature was 250 °C. The detector temperature was 260 °C with hydrogen, air, and make-up flow rates of 35, 350, and 30 mL/min, respectively. The helium (carrier gas) flow rate was 3.0 mL/min. The samples were injected in the splitless mode.

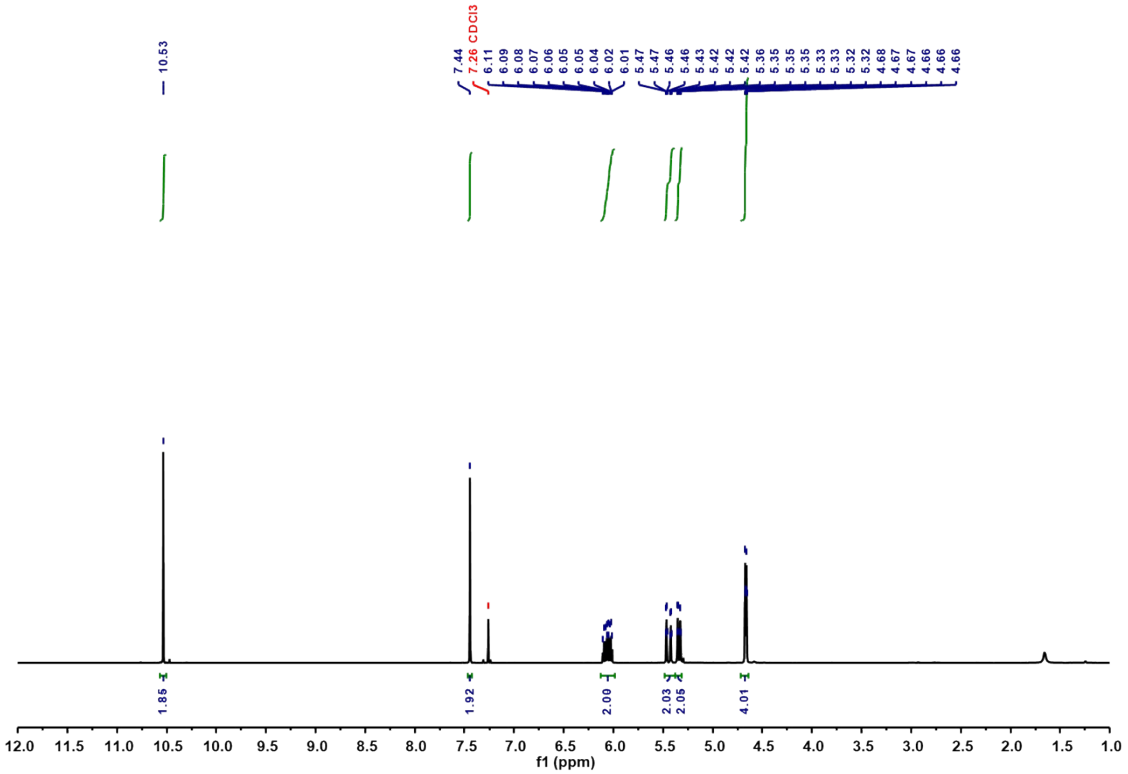


**Figure S1.** $^{1}$H NMR spectrum (400 MHz, 298K, CDCl3) of ligand **Da-A**.

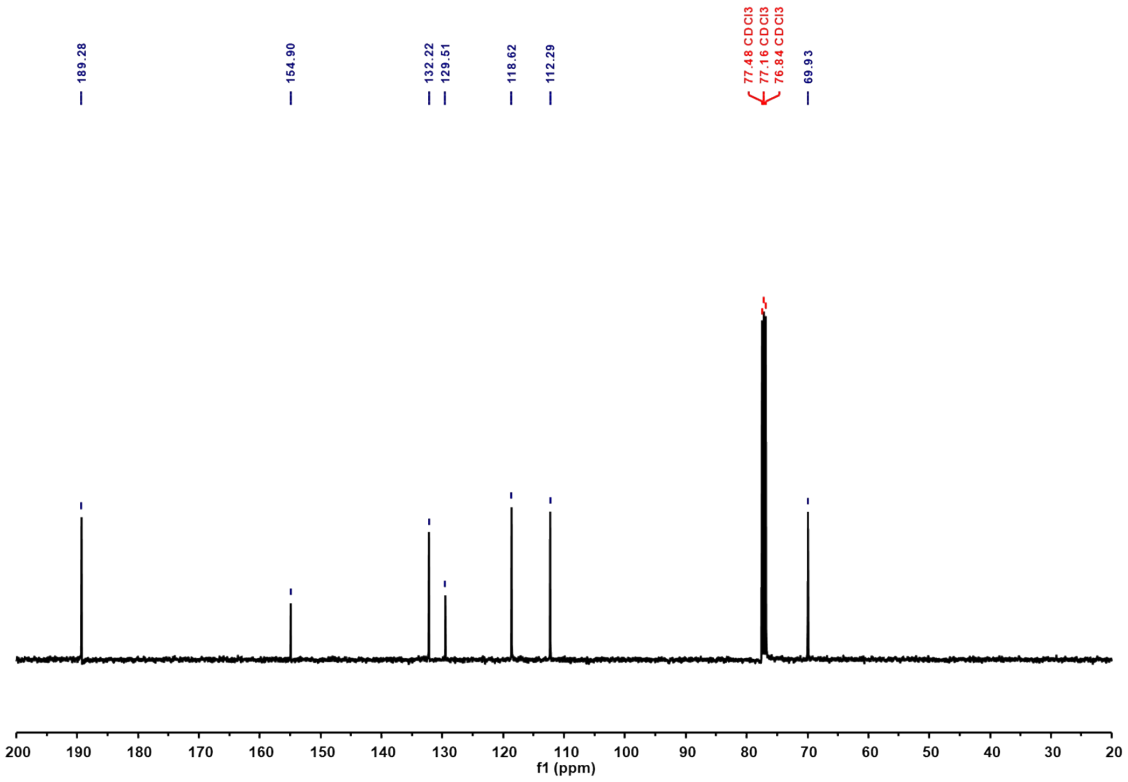


**Figure S2.** $^{13}$C NMR spectrum (101 MHz, 298K, $CDCl_3$) of ligand **Da-A**.

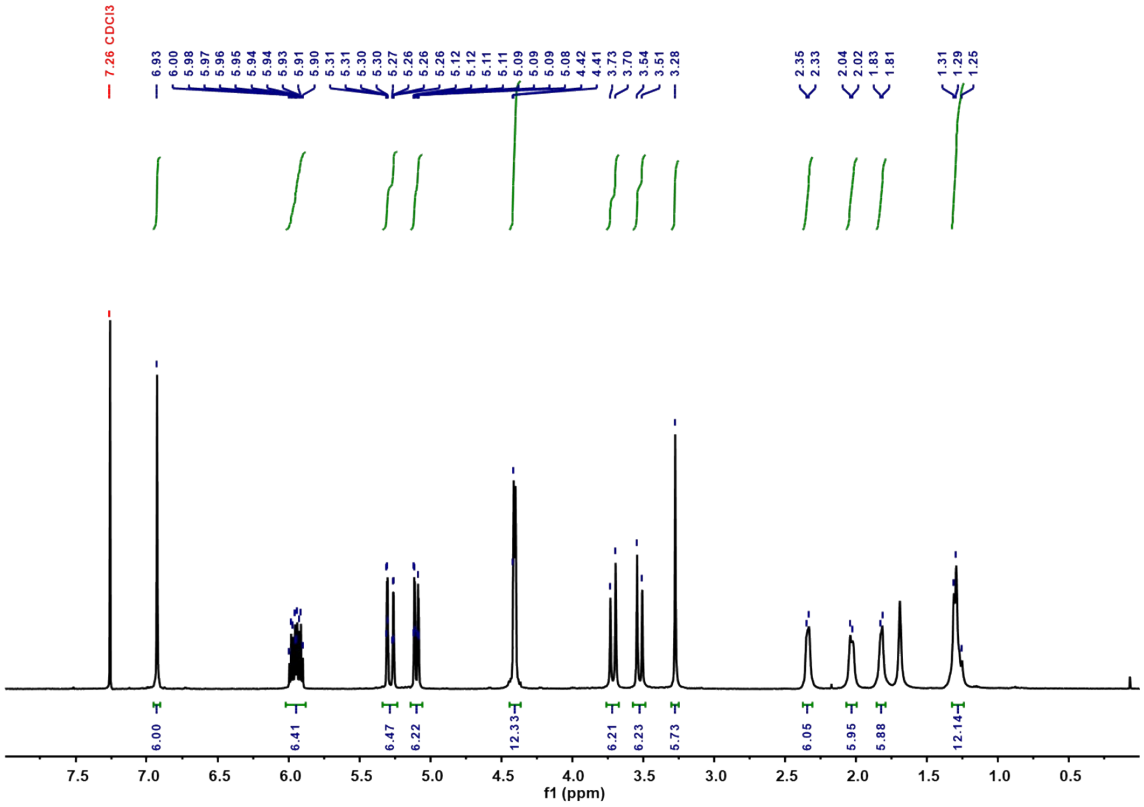


**Figure S3.** $^{1}H$ NMR spectrum (400 MHz, 298K, $CDCl_3$) of pillar[3]trianglamine **P-TA**.

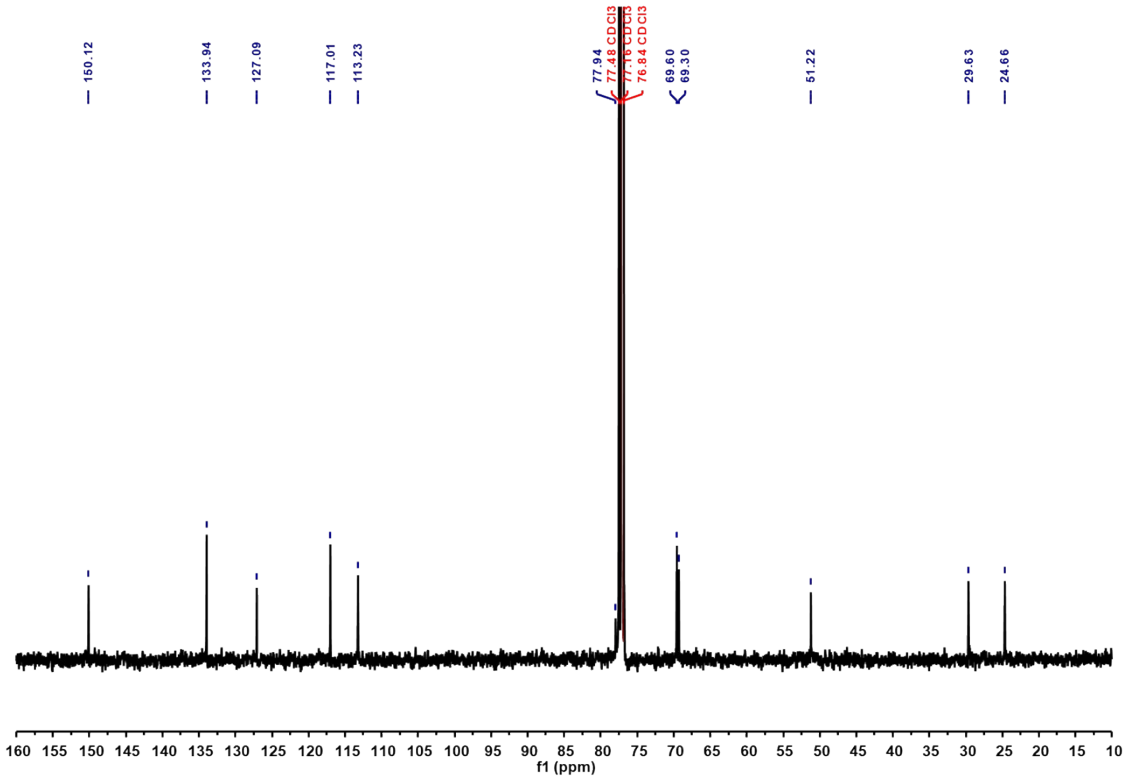


**Figure S4.** $^{13}C$ NMR spectrum (101 MHz, 298K, $CDCl_3$) of pillar[3]trianglamine **P-TA**.

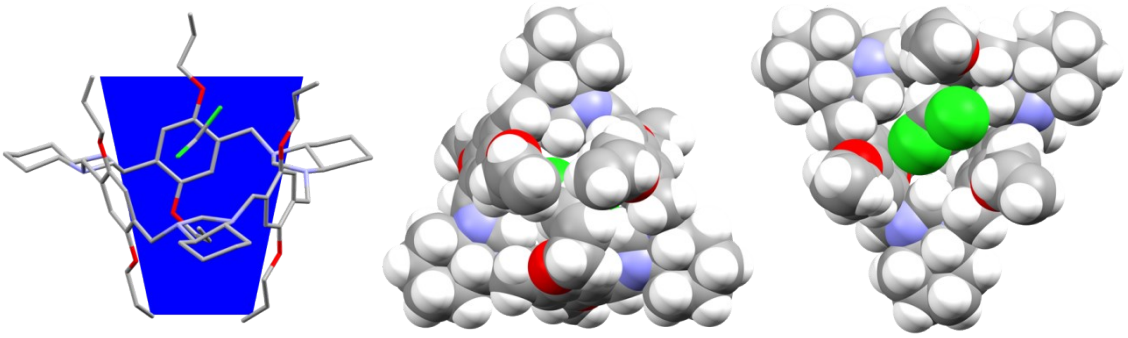

**Figure S5.** The asymmetric unit and the space filling structure of crystalline **P-TA**.

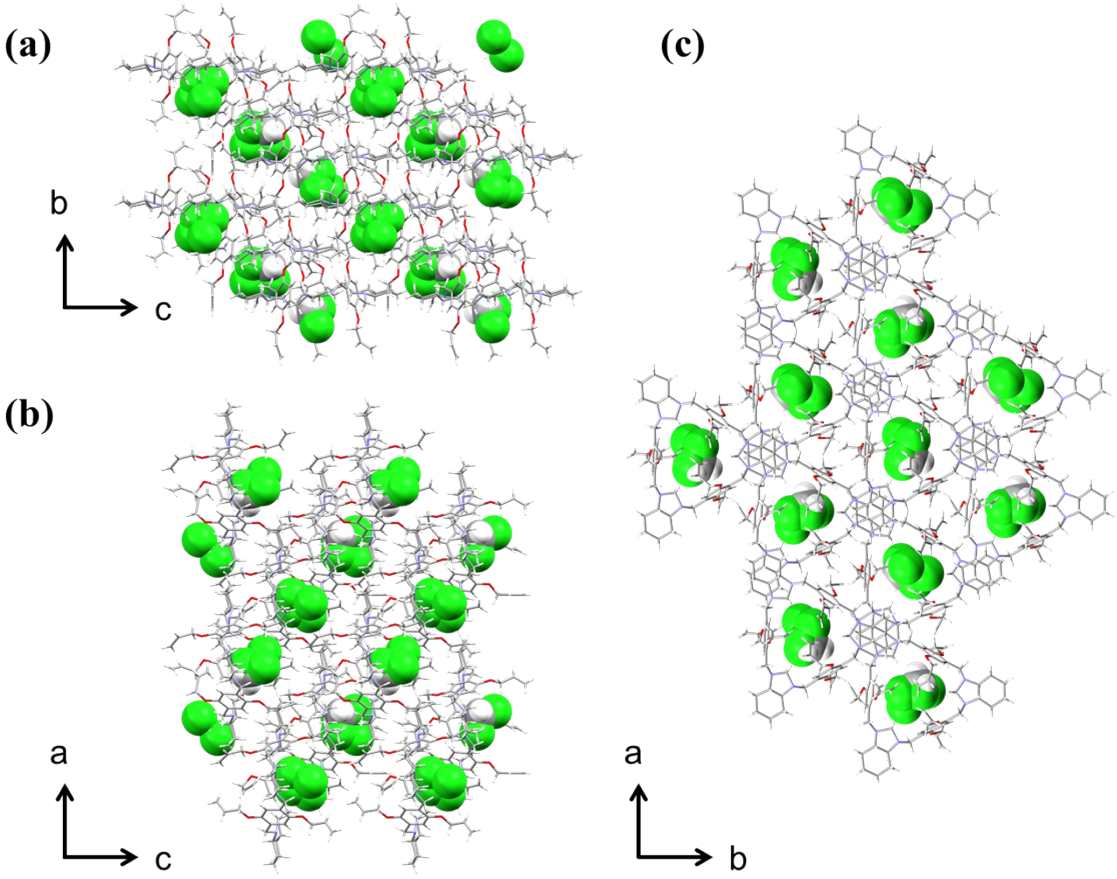


**Figure S6.** Packing arrangement of crystalline **P-TA** along (a) *a*-axis (b) *b*-axis and (c) *c*-axis.

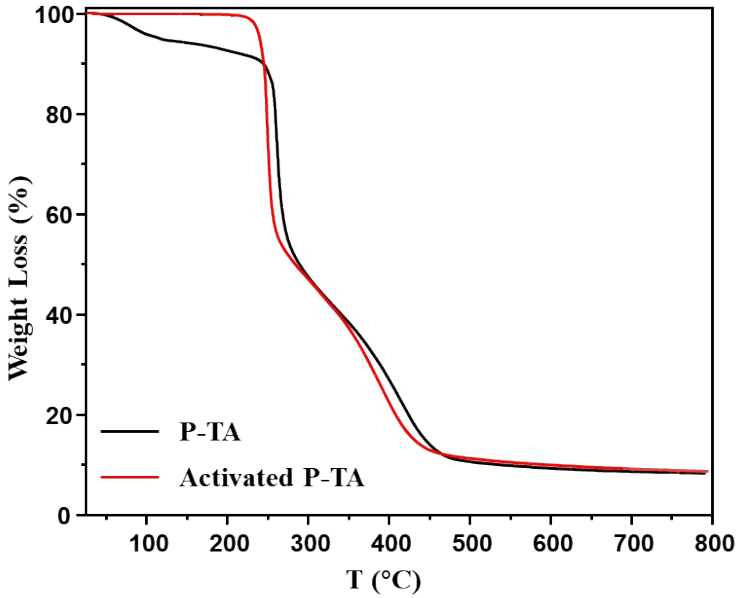


**Figure S7.** Thermogravimetric analysis: the as synthesized crystalline **P-TA** and activated **P-TA**.

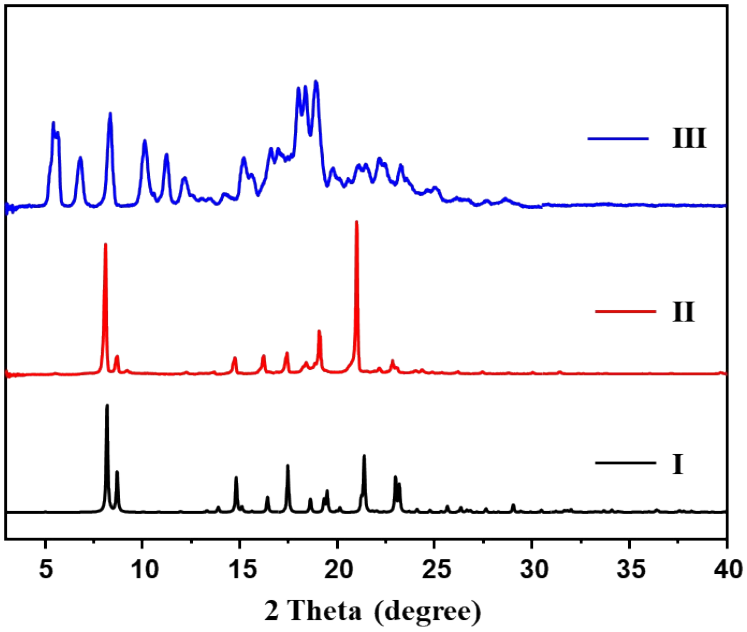


**Figure S8.** The PXRD patterns: (I) simulated from the single crystal structure of **P-TA**; (Ⅱ) experimental from **P-TA** crystals; (Ⅲ) activated **P-TA**.

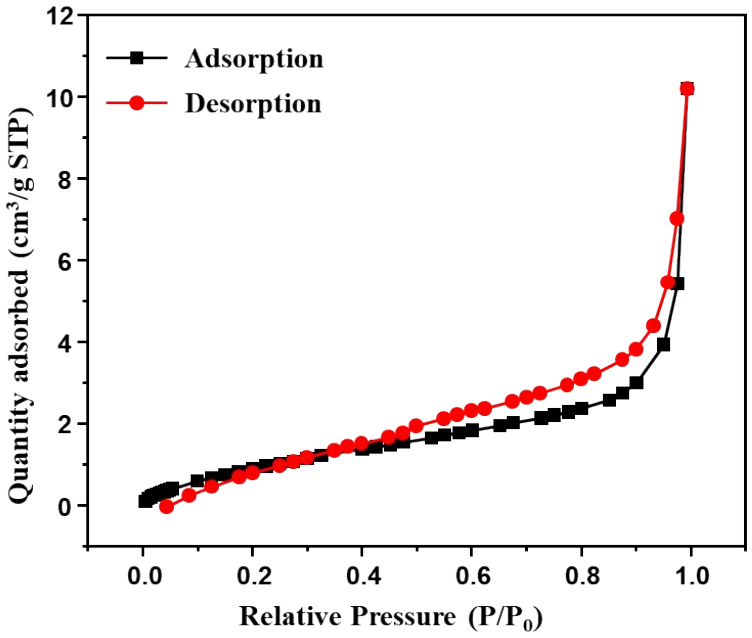


**Figure S9.** Nitrogen adsorption isotherm at 77 K for activated **P-TA**. The calculated BET surface area is 3.9 $m^2/g$.

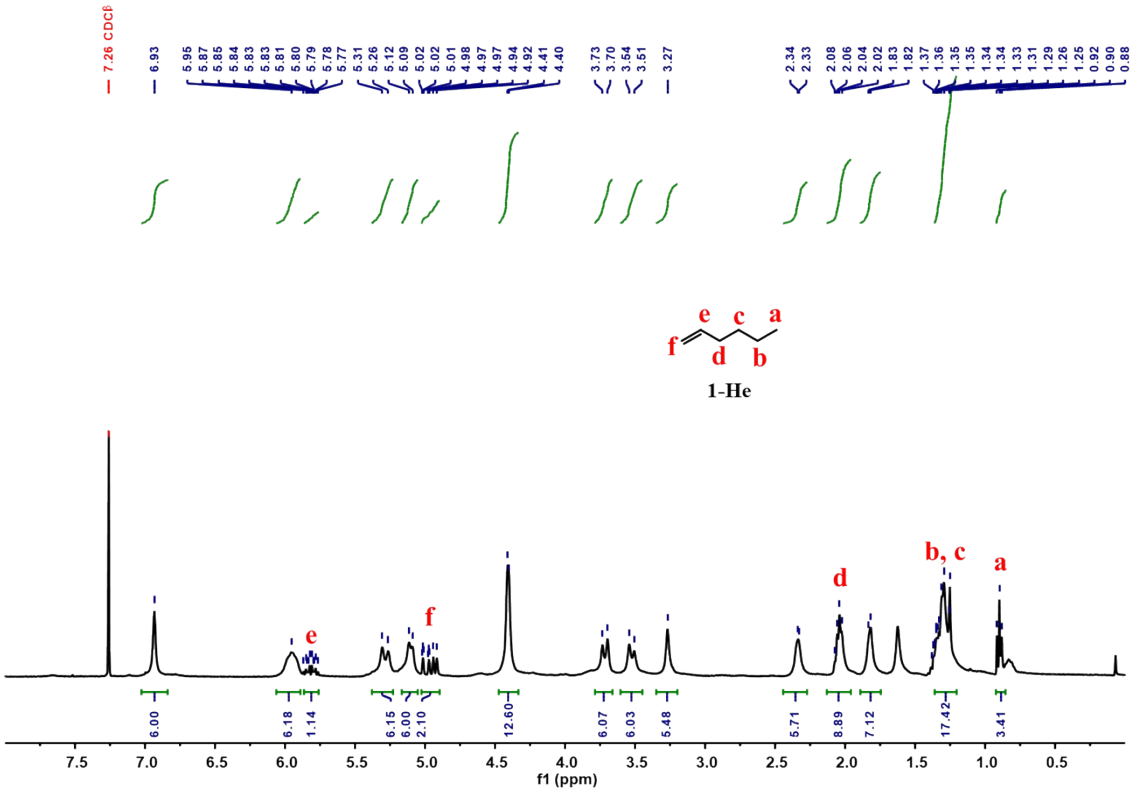


**Figure S10.** $^1H$ NMR spectra (400 MHz, chloroform-d, 298 K) of activated **P-TA** after adsorption of 1-He for 16 h.

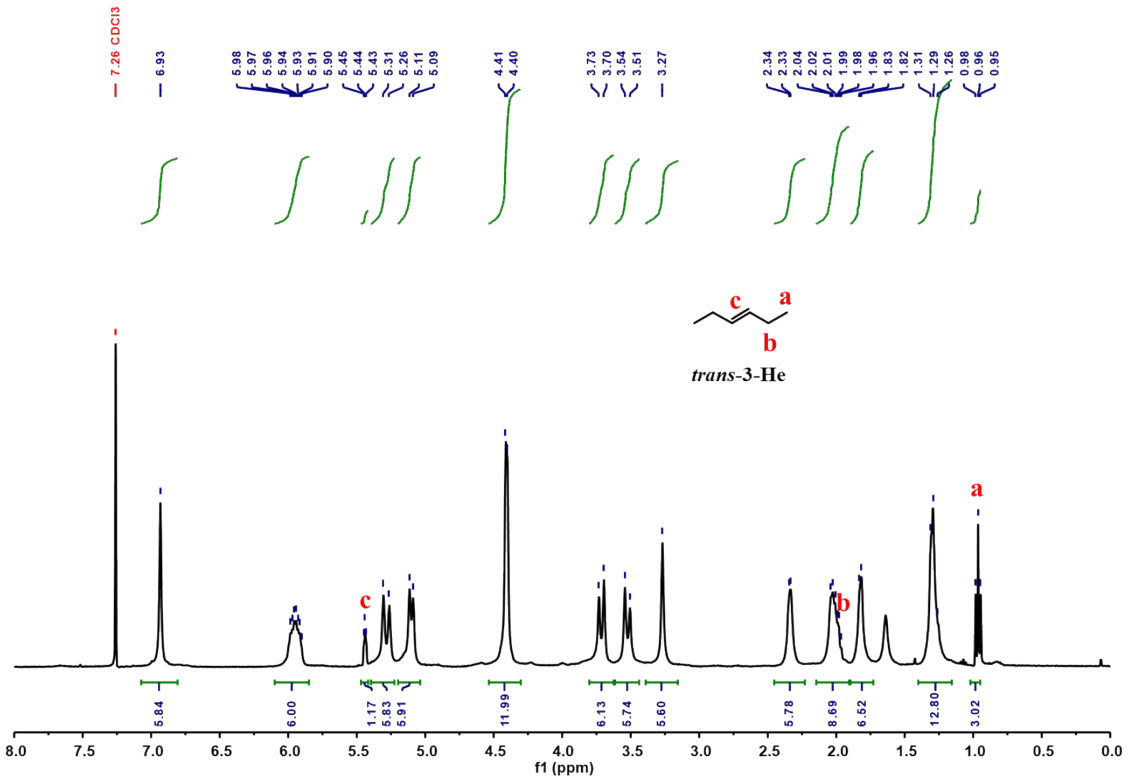


**Figure S11.** $^{1}$H NMR spectra (400 MHz, chloroform-d, 298 K) of activated **P-TA** after adsorption of *trans*-3-He for 16 h.

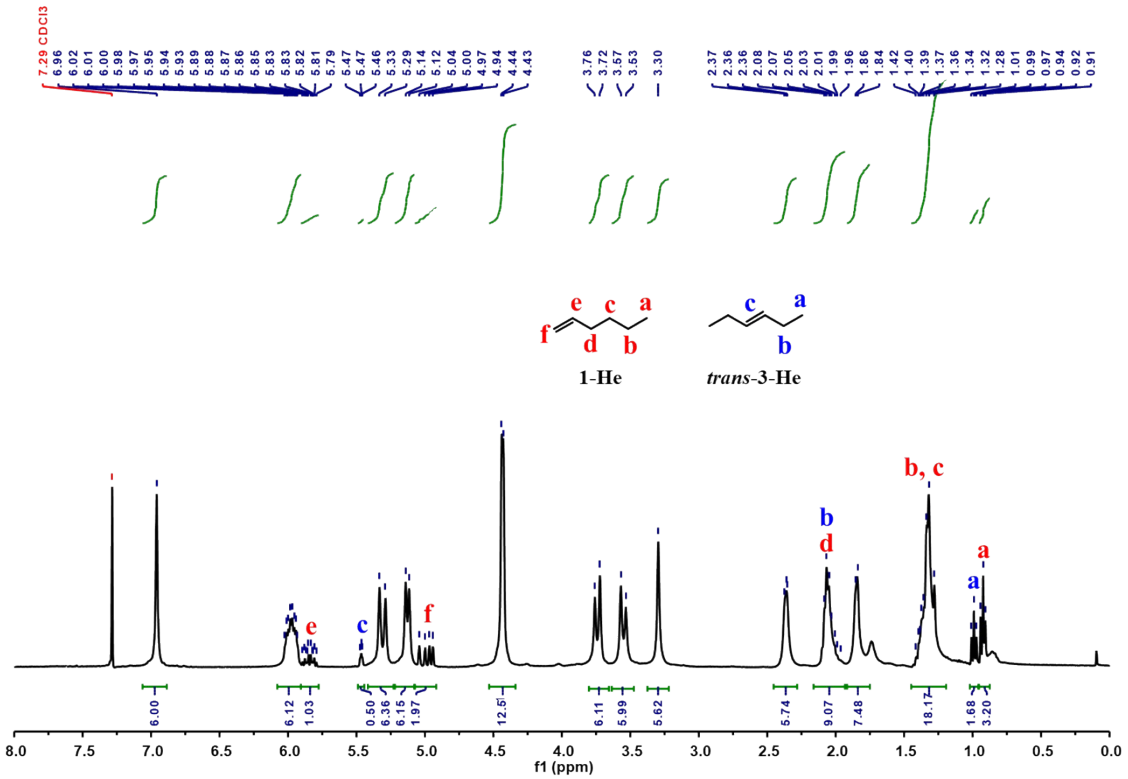


**Figure S12.** $^{1}$H NMR spectra (400 MHz, chloroform-d, 298 K) of activated **P-TA** after adsorption of 1-He/*trans*-3-He mixtures for 16 h.

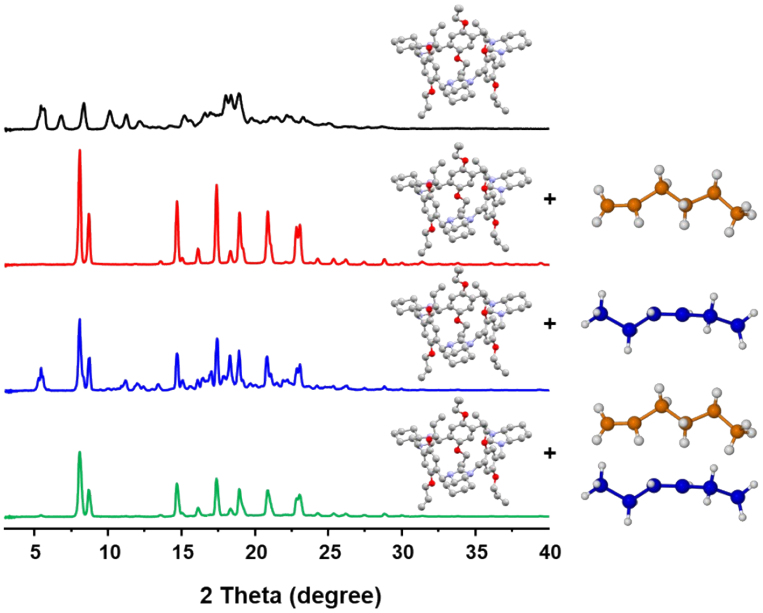


**Figure S13.** Experimental PXRD patterns of activated **P-TA** (black); activated **P-TA** after being exposed to 1-He (red); activated **P-TA** after being exposed to *trans*-3-He (blue); activated **P-TA** after being exposed to 1-He/*trans*-3-He mixtures for 16 h (green).

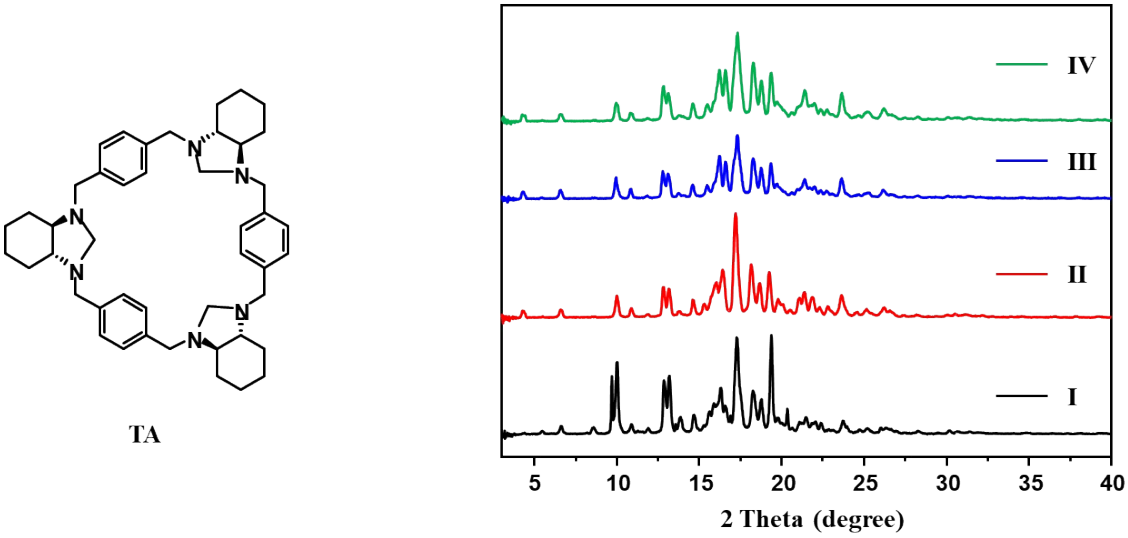


**Figure S14.** Chemical structure of **TA** and experimental PXRD patterns of (I) activated **TA**; (II) activated **TA** after being exposed to 1-He; (III) activated **TA** after being exposed to *trans*-3-He; (IV) activated **TA** after being exposed to 1-He/*trans*-3-He mixtures for 16h.

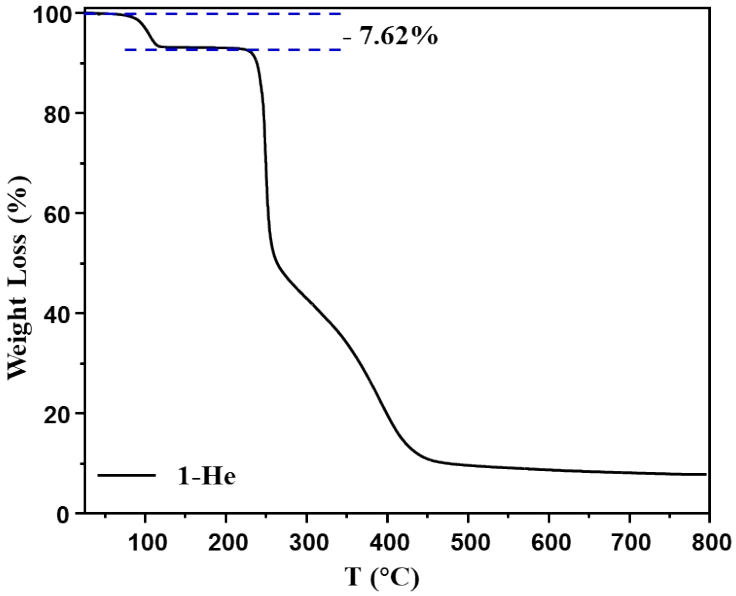


**Figure S15.** Thermogravimetric analysis of activated **P-TA** after adsorption of 1-He.

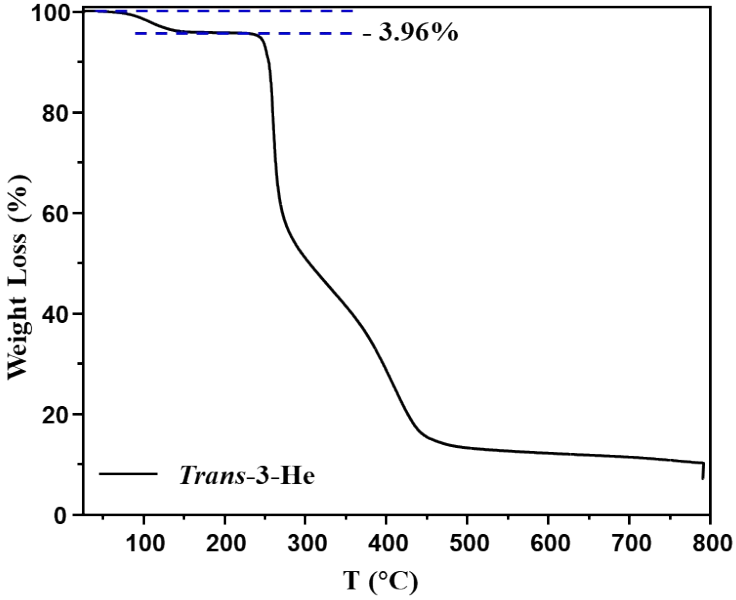


**Figure S16.** Thermogravimetric analysis of activated **P-TA** after adsorption of *trans*-3-He.

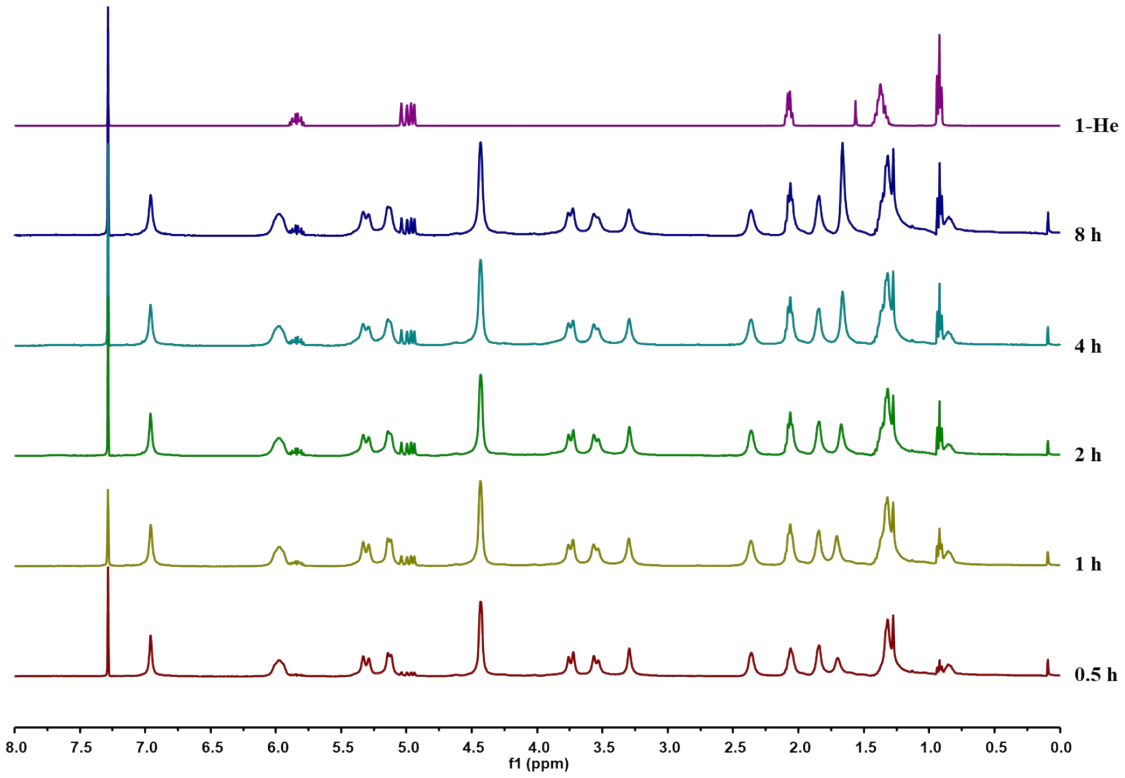


**Figure S17.** $^{1}$H NMR spectra (400 MHz, chloroform-d, 298 K) of activated **P-TA** after adsorption of 1-He over time.

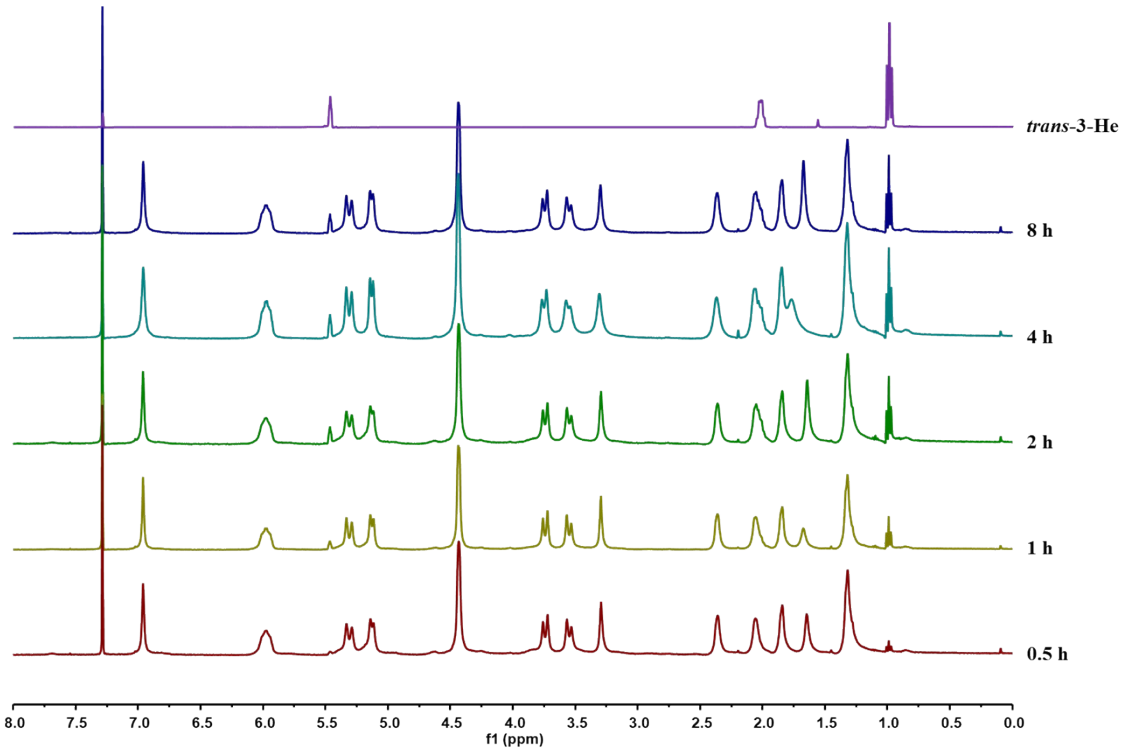


**Figure S18.** $^{1}$H NMR spectra (400 MHz, chloroform-d, 298 K) of activated **P-TA** after adsorption of *trans*-3-He over time.

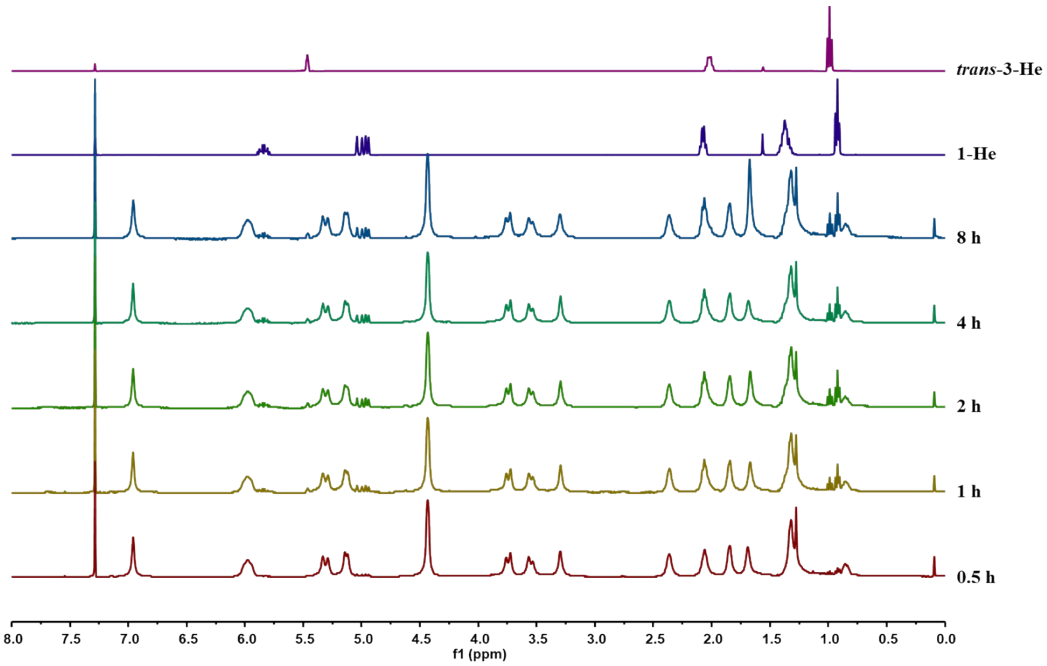


**Figure S19.** $^{1}$H NMR spectra (400 MHz, chloroform-d, 298 K) of activated **P-TA** after adsorption of 1-He/*trans*-3-He mixtures over time.

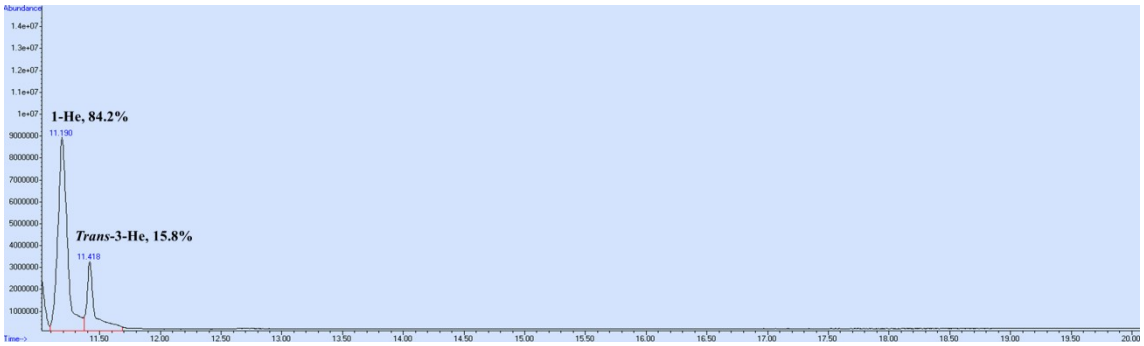


**Figure S20.** Gas chromatography showing the relative uptake of 1-He and *trans*-3-He by activated **P-TA** from their mixtures for 16h.

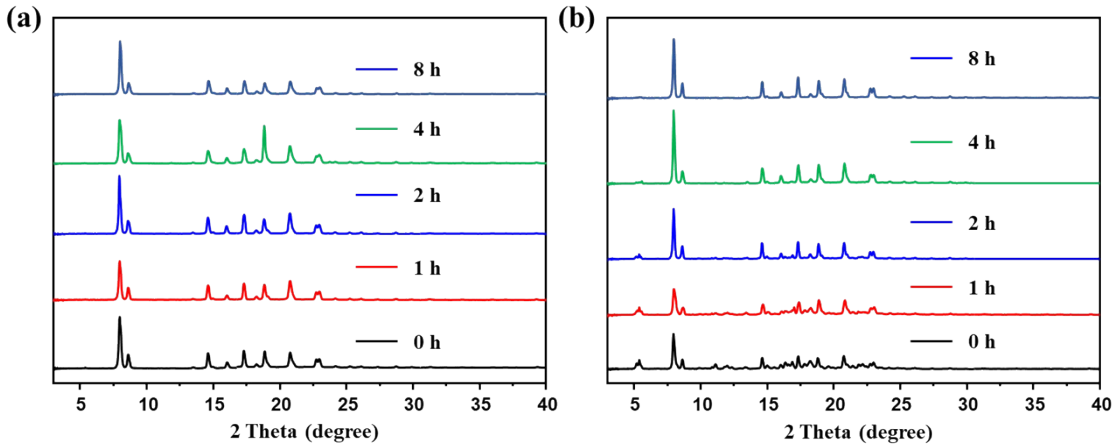


**Figure S21.** (a) Time-dependent PXRD patterns of **P-TA** loaded with 1-He after exposure to *trans*-3-He vapor under different times. (b) Time-dependent PXRD patterns of **P-TA** loaded with *trans*-3-He after exposure to 1-He vapor under different times.

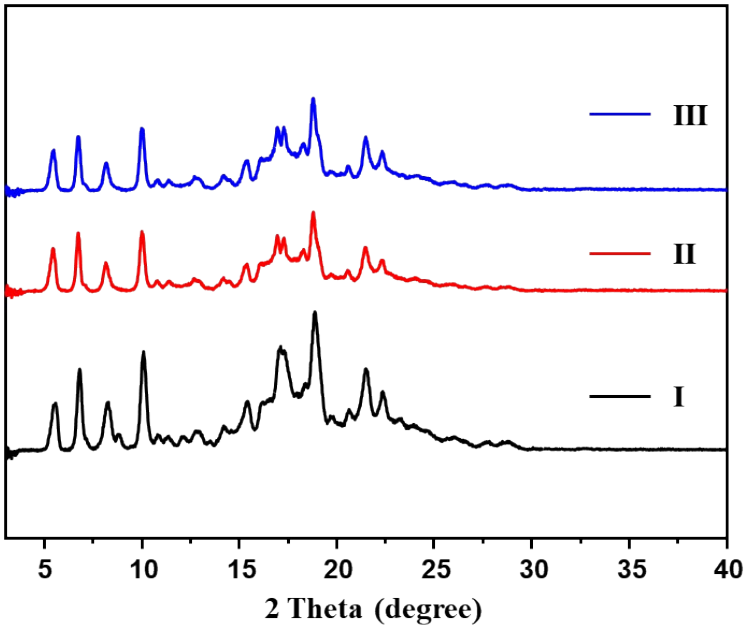


**Figure S22.** Experimental PXRD patterns of guest-loaded **P-TA** (exposing to 1-He and *trans*-3-He mixtures) after guests were fully removed at 90 °C under vacuum: (I) the first cycle; (II) the third cycle; (III) the fifth cycle.

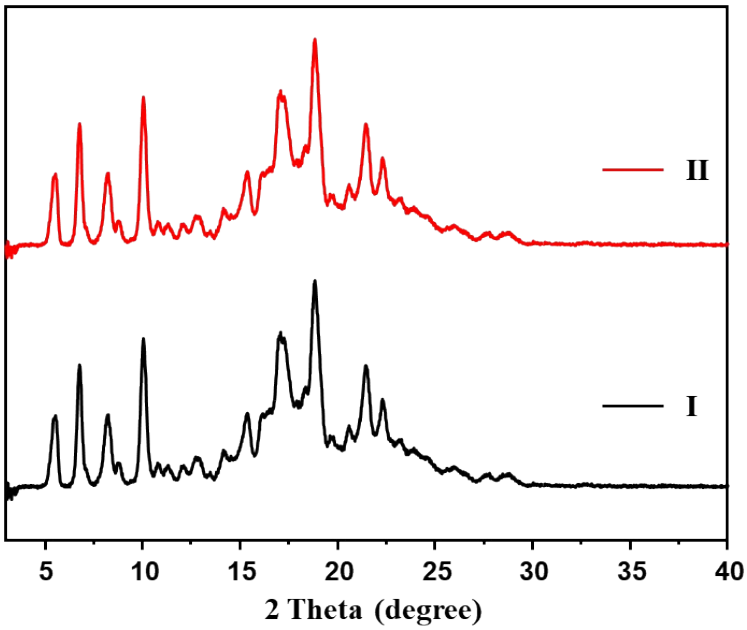


**Figure S23.** Water stability of: (I) activated **P-TA**; (II) activated **P-TA** soaked in water for 7 days.

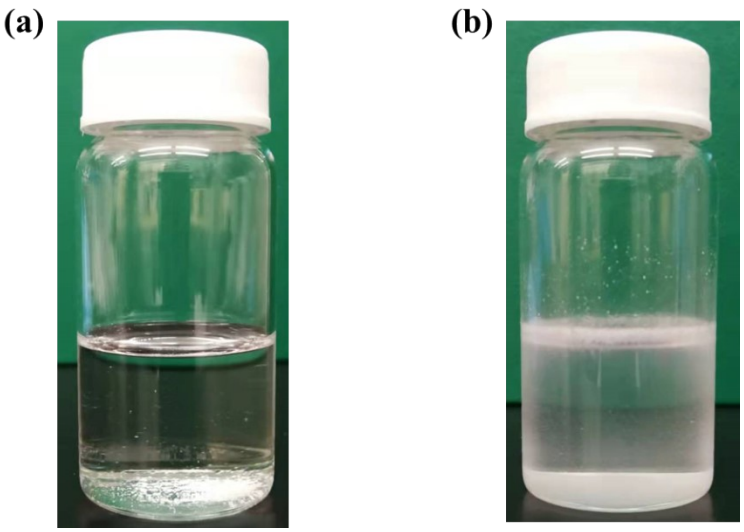


**Figure S24.** Activated **P-TA** (1mg) in 1-He (10 mL) (a) before and (b) after sonication for 10 min.

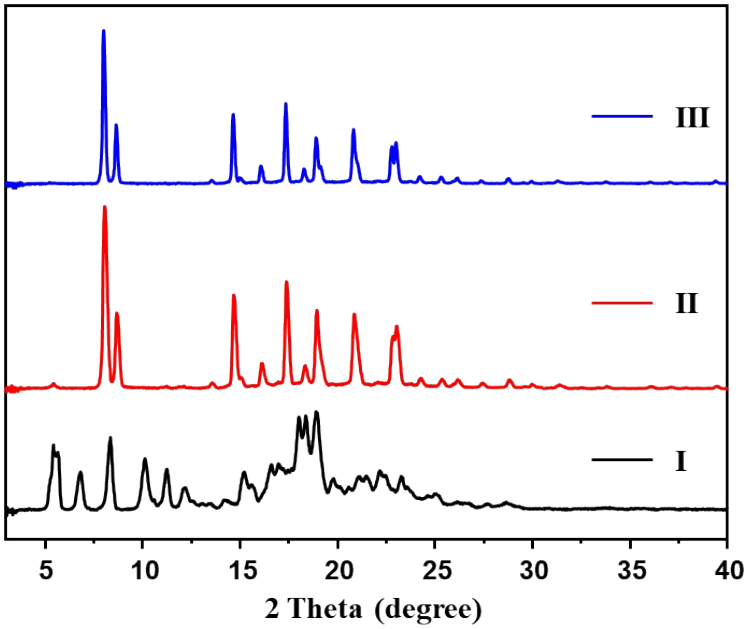


**Figure S25.** Experimental PXRD patterns of activated **P-TA** after exposure to 1-He/*trans*-3-He mixtures for 16 h: (I) activated **P-TA**; (II) activated **P-TA** in vapor; (III) activated **P-TA** in liquid.

***Synthesis of SBA-15.*** SBA-15 was prepared according to a previously published report.[6]

***Synthesis of modified SBA-15.*** Activated **P-TA** (150 mg) was firstly dissolved in DCM (10 mL), then SBA-15 (150mg) was added into the above solution. The mixture was then sonicated followed by slow evaporation of dichloromethane and washing by DCM (3 times). The as-synthesized **P-TA** loaded SBA-15 was finally dried under vacuum at 120 ℃ overnight.

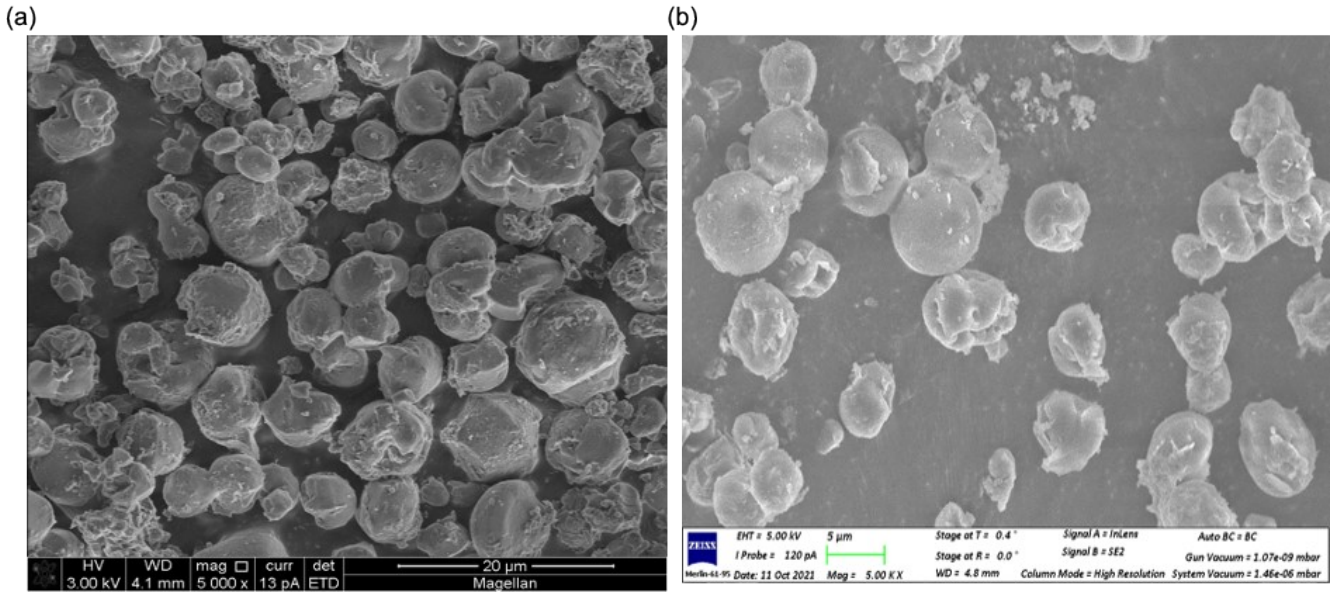


**Figure S26.** SEM images (a) SBA-15; (b) **P-TA** modified SBA-15 showing no **P-TA** crystallization on the surface.

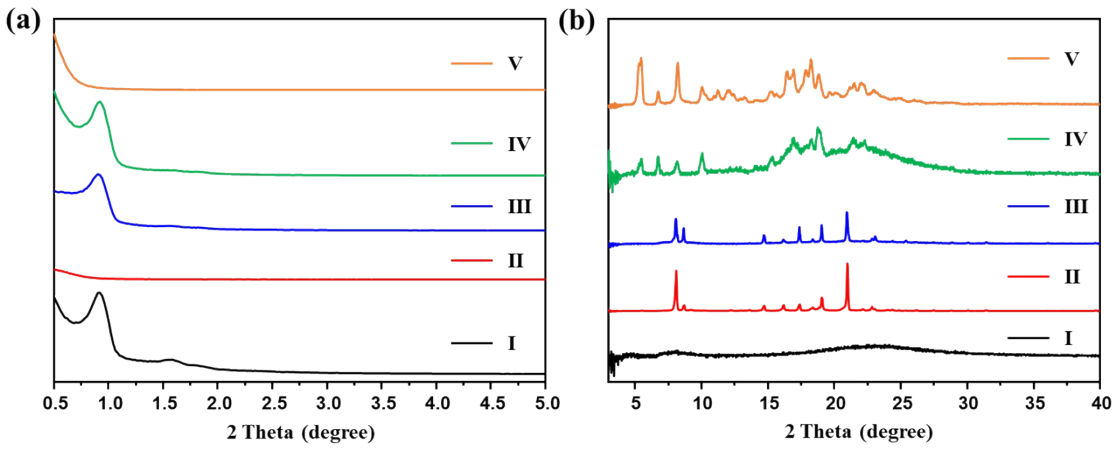


**Figure S27.** (a) small-angle and (b) broad-angle PXRD patterns: (I) SBA-15; (II) **P-TA** crystals; (III) as-synthesized **P-TA** loaded SBA-15; (IV) modified SBA-15; (V) activated **P-TA.**

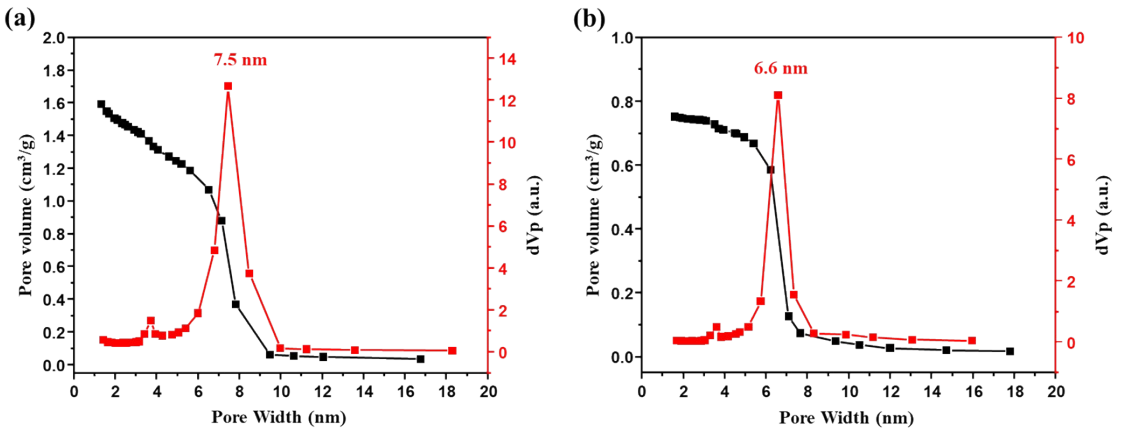


**Figure S28.** Pore size distributions of (a) SBA-15 and (b) modified SBA-15.

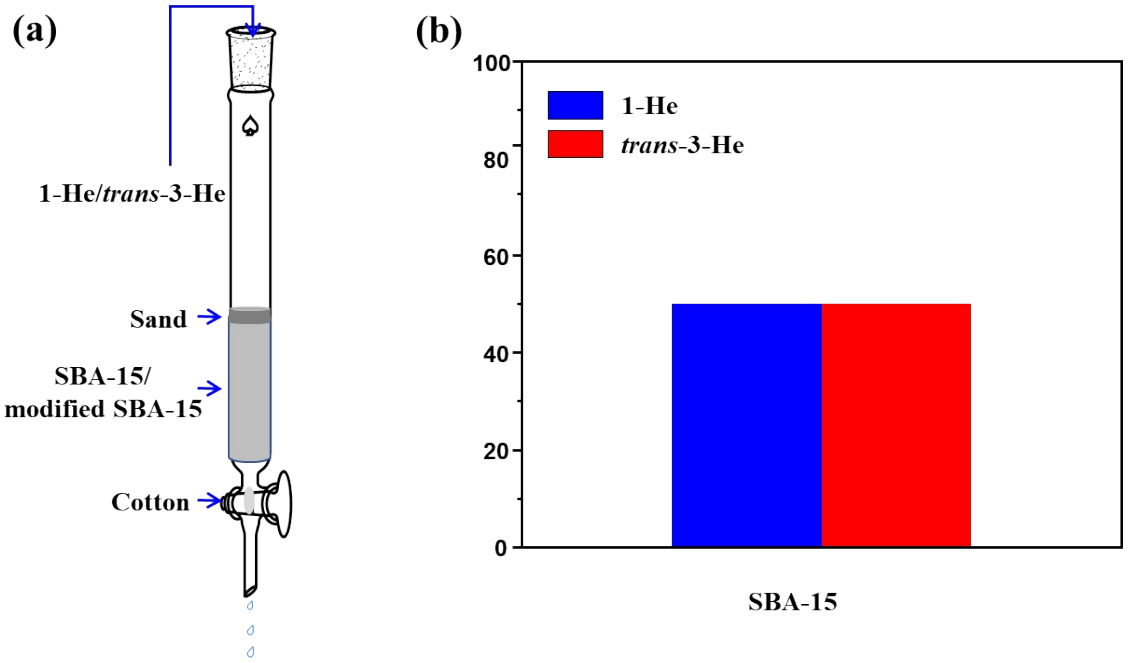


**Figure S29.** (a) Setup of column chromatography using SBA-15 or modified SBA-15 as the stationary phase. (b) Relative amount of 1-He and *trans*-3-He after the first run with unmodified SBA-15 as the stationary phase.

**Table S1**. Experimental single crystal X-ray data.

| Identification code | **TA** | **P-TA** |
|---|---|---|
| Empirical formula | $C_{45}H_{60}N_6 \cdot CH_2Cl_2$[a] | $C_{63}H_{84}N_6O_6 \cdot CH_2Cl_2$[a] |
| Formula weight | 769.91 | 1106.28 |
| Temperature /K | 120.05 | 120.0 |
| Crystal system | Orthorhombic | Trigonal |
| Space group | *P* $2_12_12_1$ | *P* 31 |
| a /Å | 9.0657(2) | 20.2894(6) |
| b /Å | 18.4002(4) | 20.2894(6) |
| c /Å | 25.5482(5) | 13.6577(5) |
| α /° | 90.00 | 90.00 |
| β /° | 90.00 | 90.00 |
| γ /° | 90.00 | 120.00 |
| Volume /Å$^3$ | 4261.71(16) | 4869.1(3) |
| Z | 4 | 3 |
| $\rho_{calc}$ g/cm$^3$ | 1.200 | 1.132 |
| μ /mm$^{-1}$ | 0.192 | 0.151 |
| F(000) | 1656 | 1782 |
| Radiation | MoKα (λ = 0.71073Å) | MoKα (λ = 0.71073Å) |
| Theta range for data collection/° | 2.35 to 27.45 | 2.32 to 27.09 |
| Index ranges | $-11 \le h \le 11$, $-23 \le k \le 23$, $-31 \le l \le 33$ | $-26 \le h \le 21$, $-26 \le k \le 26$, $-17 \le l \le 17$ |
| Reflections collected | 39169 | 63281 |
| Independent reflections | 9752 [$R_{int}$ = 0.0368, $R_{sigma}$ = 0.0325] | 14887 [$R_{int}$ = 0.0667, $R_{sigma}$ = 0.0533] |
| Data/restraints/parameters | 8444/44/514 | 11228/117/731 |
| Goodness-of-fit on F$^2$ | 1.048 | 1.052 |
| Final R indexes [I>=2σ (I)][b] | $R_1$ = 0.0447, $wR_2$ = 0.1044 | $R_1$ = 0.0699, $wR_2$ = 0.1820 |
| Final R indexes [all data][b] | $R_1$ = 0.0572, $wR_2$ = 0.1147 | $R_1$ = 0.1001, $wR_2$ = 0.2123 |
| CCDC | 2113421 | 2115290 |

[a] Formula is given based on single-crystal X-ray data.
[b] $R_1 = \Sigma||F_o| - |F_c||/ \Sigma|F_o|$, $wR_2 = \{ \Sigma[w(F_o^2-F_c^2)^2]/ \Sigma[w(F_o^2)^2]\}^{½}$

**Table S2**. Experimental single crystal X-ray data.

| Identification code | **1-He@P-TA** | ***trans*-3-He@P-TA** |
|---|---|---|
| Empirical formula | $C_{63}H_{84}N_6O_6 \cdot C_6H_{12}$[a] | $C_{63}H_{84}N_6O_6 \cdot 0.5(C_6H_{12})$[a] |
| Formula weight | 1105.51 | 1063.43 |
| Temperature /K | 120.0 | 120.0 |
| Crystal system | Trigonal | Trigonal |
| Space group | *R 3* | *R 3* |
| a /Å | 20.366 | 20.3338(3) |
| b /Å | 20.366 | 20.3338(3) |
| c /Å | 13.791 | 13.7372(4) |
| α /° | 90.00 | 90.00 |
| β /° | 90.00 | 90.00 |
| γ /° | 120.00 | 120.00 |
| Volume /Å$^3$ | 4953.9 | 4918.9(2) |
| Z | 3 | 3 |
| $\rho_{calc}$ g/cm$^3$ | 1.112 | 1.077 |
| μ /mm$^{-1}$ | 0.553 | 0.540 |
| F(000) | 1800 | 1728 |
| Radiation | CuKα (λ = 1.54178 Å) | CuKα (λ = 1.54178 Å) |
| Theta range for data collection/° | 4.344 to 65.024 | 5.97 to 65.10 |
| Index ranges | -23≤ h ≤23, -23≤ k ≤ 23, -16 ≤l ≤ 16 | -22≤ h ≤23, -23≤ k ≤ 23, -16 ≤l ≤ 16 |
| Reflections collected | 16121 | 21516 |
| Independent reflections | 3722 [$R_{int}$ = 0.0241, $R_{sigma}$ = 0.0206] | 3648 [$R_{int}$ = 0.0215, $R_{sigma}$ = 0.0145] |
| Data/restraints/parameters | 3721/1049/282 | 3650/908/283 |
| Goodness-of-fit on F$^2$ | 1.102 | 1.074 |
| Final R indexes [I>=2σ (I)][b] | $R_1$ = 0.0381, $wR_2$ = 0.1073 | $R_1$ = 0.0708, $wR_2$ = 0.2055 |
| Final R indexes [all data][b] | $R_1$ = 0.0381, $wR_2$ = 0.1073 | $R_1$ = 0.0708, $wR_2$ = 0.2056 |
| CCDC | 2120030 | 2113573 |

[a] Formula is given based on single-crystal X-ray data.
[b] $R_1 = \Sigma||F_o| - |F_c||/ \Sigma|F_o|$, $wR_2 = \{ \Sigma[w(F_o^2-F_c^2)^2]/ \Sigma[w(F_o^2)^2]\}^{½}$

# Reference


[1] Hua, B.; Ding, Y.; Alimi, L.; Moosa, B.; Zhang, G.; Sessler, J. L.; Khashab, N. M. *Chem. Sci.* **2021**, *12*, 12286–12291.

[2] Jie, K.; Liu, M.; Zhou, Y.; Little, M. A.; Bonakala, S.; Chong, S. Y.; Stephenson, A.; Chen, L.; Huang, F.; Cooper, A. I. *J. Am. Chem. Soc.* **2017**, *139*, 2908–2911.

[3] SAINT. Bruker AXS. Inc, Madison, Wisconsin, USA, **2014**.

[4] SADABS. G. M. Sheldrick, University of Gottingen, Germany, **2008**.

[5] Sheldrick, G. M. A Short History of SHELX. *Acta Crystallogr.* **2008**, *A64*, 112–122.

[6] Chaudhary, V., Sharma, S. *J. Porous Mater.* **2017**, *24*, 741-749.